TRACE METAL RETENTION IN LBOS-AMENDED, VERTICAL-FLOW CONSTRUCTED WETLANDS TREATING LOW PH, FERRIC IRON-DOMINATED ACID ROCK DRAINAGE[1]

Robert C. Thomas, Christopher S. Romanek, and Lindy S. Paddock [2]

Abstract. Remediation strategies employed for mitigation of low-pH, metal-sulfate drainage (i.e., acid rock drainage, ARD) may include passive treatment systems. While shown effective for neutralization of acid and removal of major ions (e.g., iron, aluminum, and manganese), trace element removal during acid neutralization in passive systems is rarely investigated. Therefore, in this presentation, we will focus on the fate of trace metals in one common type of passive treatment system, the vertical flow wetland (VFW). Our experimental VFW contained a limestone buffered organic substrate (LBOS) and received low pH (<3), ferric iron-dominated ARD for two years. During this time, trace elements (As, Cd, Cr, Cu, U, Co, Ni, and Zn) were removed along a pH gradient controlled by a series of reaction zones that developed above a dynamic limestone dissolution front. Therefore, for the practical purpose of implementing LBOS to treat low pH, ferric iron-dominated ARD, high trace element removal efficiency can be expected as long as the limestone dissolution front does not pass completely through the substrate. With the exception of uranium, trace metal attenuation largely occurred above the limestone dissolution front in the transitional and oxide reaction zones. Moreover, trace metal removal exhibited a strong dependence on pH. Based largely on increasing pH with depth, trace metal removal within the LBOS follows the sequence:

$$As > Cu > Cr > Co = Ni = Zn = Cd > U.$$

Cadmium, copper, chromium, cobalt, nickel, zinc, and uranium were subject to remobilization as the pH decreased over time, although the degree of mobilization was trace element-dependent; arsenic was not remobilized. The following general order of trace element mobility can be applied to the LBOS:

$$U > Co = Zn \geq Cd = Ni > Cu > Cr > As.$$

Additional Key Words: trace element removal, sorption selectivity, arsenic, cadmium, chromium, copper, uranium, cobalt, nickel, zinc.

---

[1]Paper was presented at the 2004 National Meeting of the American Society of Mining and Reclamation and The 25th West Virginia Surface Mine Drainage Task Force, April 18-24, 2004. Published by ASMR, 3134 Montavesta Rd., Lexington, KY 40502.

[2] Robert C. Thomas is currently a Federal Post Doctoral Associate, US EPA/NERL/Ecosystems Research Division, 960 College Station Road, Athens GA 30605. This research was completed prior to his appointment with US EPA. Christopher S. Romanek is an Associate Research Scientist and Associate Professor, Savannah River Ecology Laboratory and Department of Geology, University of Georgia, PO Drawer E, Aiken, SC 29802. Lindy S. Paddock is a Research Technician at the Savannah River Ecology Laboratory

Introduction

Passive treatment technologies, including constructed treatment wetlands, are widely used for the remediation of acid rock drainage (ARD) related to coal mining in the eastern United States. Because pH, total iron, total manganese, and total suspended solids are generally the only constituents regulated for ARD originating from coal mining activities (U.S. Code of Federal Regulations, 1991), evaluations of most passive treatment systems focus on the neutralization of acid and acid-generating contaminants, and the long-term retention of metals (e.g., iron and manganese). The ultimate fate of trace contaminants is rarely investigated despite the fact that elevated levels of some trace metals are commonly encountered in coal-related ARD (e.g., As, Cd, Co, Cr, Cu, Ni, Zn; Hyman and Watzlaf, 1997). The focus of this paper, therefore, is the fate of trace metals in low pH (<3) ferric iron-dominated ARD treated by one common type of passive system, the vertical flow wetland (VFW).

In VFWs, water flows downward by gravity, usually from a pond, through organic matter and limestone before flowing out through a drainage system. The limestone may be mixed with organic matter in a single layer (limestone buffered organic substrate or LBOS, Thomas, 2002) or the VFW may be constructed in distinct layers consisting of organic matter overlying limestone (Kepler and McCleary, 1994). When VFWs containing LBOS are used to treat low pH (<3), ferric iron-dominated ARD, acid neutralization is ultimately controlled by limestone dissolution along a fairly narrow (2 – 5 cm) front that migrates through the substrate over time (Watzlaf, 1997; Thomas, 2002). Below the dissolution front, where pore water is buffered by limestone, pH is >6.5 and dissolved metal content approximates that of the final effluent. Within and above the dissolution front, pH and metal (i.e., iron and aluminum) mobility is ultimately controlled by a series of mineral dissolution-precipitation reactions that involves carbonates, aluminum hydroxysulfates, and iron oxyhydroxides (Blowes and Ptacek, 1994; Thomas, 2002). With continued influx of ARD through the LBOS, the dissolution front will migrate through LBOS and pore water pH and metal concentration will eventually approach that of the influent.

Thomas (2002) identified a series of three mineralogical reaction zones that characterize the reaction sequence through time: the oxide, transitional, and sulfide zones (Fig. 1). Thomas (2002) described the paragenetic sequence for the development of the three reaction zones, which can be summarized as follows. The first reaction zone to develop is the sulfide zone. The

Figure 1. Photograph of a core taken from the LBOS showing the three reaction zones. Scale to the right is in centimeters.

Sulfide zone is characterized by ubiquitous iron sulfides (e.g., pyrite), pristine limestone, and

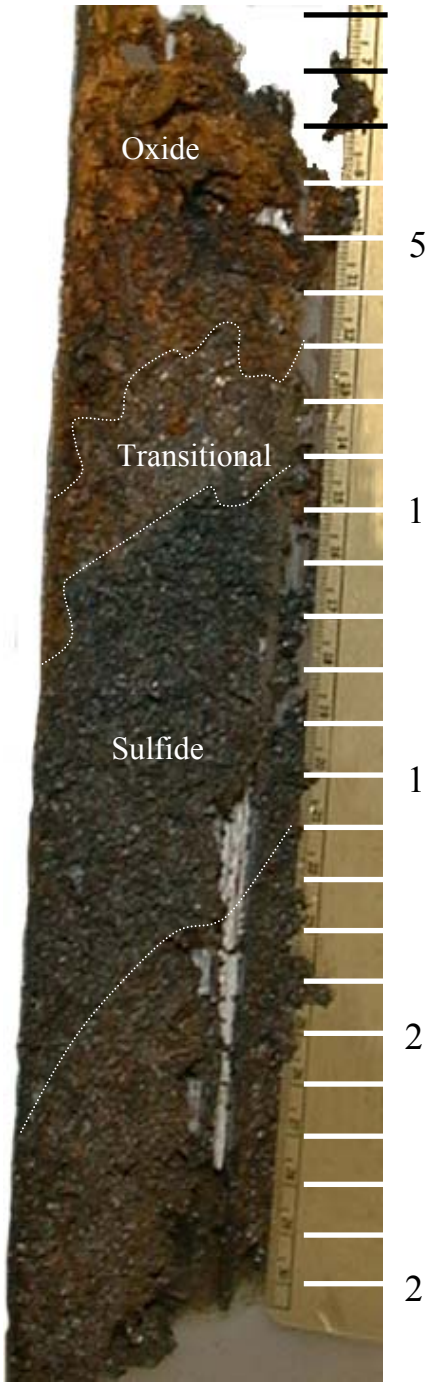

pore water near calcite saturation; it develops below the dissolution front where pore water pH is > 6.5. The sulfide zone is dynamic, "rolling" ahead of the limestone dissolution front as it

advances. However, the sulfide zone is ephemeral in nature. At any fixed position within the sulfide zone, with the advancement of the limestone dissolution front, the sulfide zone is overprinted by a transitional zone. The transitional zone, which is defined by partially dissolved limestone and abundant aluminum and calcium hydroxysulfates, demarcates the advancing limits where limestone dissolution occurs. The pore water pH of the transitional zone is held steady between 3.8 and 4.6 by the dissolution of limestone and the precipitation of aluminum and calcium hydroxysulfates. Concurrent with the drop in pH, acid volatile sulfides of the sulfide zone are solubilized and leached while less reactive sulfides, such as pyrite remains. Similar to the sulfide zone, the transitional zone is also both dynamic and ephemeral, advancing with the limestone dissolution front while being overprinted by an overlying oxide zone. Encroachment of the oxide zone, which contains abundant iron oxyhydroxides and only minor aluminum hydroxysulfate in the lower portions, occurs as limestone is consumed completely within the transitional zone. Without the buffering capacity of limestone, pore water pH in the upper transitional – lower oxide zones drops and previously precipitated aluminum and calcium hydroxysulfates dissolve. Thus, the pore water pH of the oxide zone is held at a pH between the influent value and 3.8 by the dissolution of aluminum and calcium hydroxysulfates and the precipitation of iron oxyhydroxides. As part of the overprinting process, pyrite generated in the sulfide zone is dissolved in the oxide zone by ferric iron oxidation of the sulfide moeity. Moreover, aluminum and calcium hydroxysulfates dissolved in the oxide zone are reprecipitated in the advancing transitional zone (Thomas, 2002).

Thus, the oxide zone represents the final stage of LBOS evolution; all of the original limestone, as well as secondary aluminum and calcium hydroxysulfates and iron sulfides, have been removed. Previous studies (Watzlaf, 1997; Thomas, 2002) have suggested that, given enough time, the limestone dissolution front will eventually migrate completely through the organic layer and the entire column of substrate will eventually experience the breadth of reactions that culminate in the conversion of the LBOS to “oxide zone” material. Hence, trace metals retained in the oxide zone may be sequestered permanently, whereas trace metals removed in the transitional and sulfide zones, but solubilized in the oxide zone may represent transient retention and result in delayed release from the VFW. Based on this model, determining the ultimate trace element retaining capacity of the LBOS should be as simple as determining the total trace element content sequestered in the oxide zone.

The primary objectives of this study were: (1) to characterize the vertical distribution of As, Cr, Cu, Co, Ni, U, and Zn dissolved in pore water and retained as solids within the three reaction zones of LBOS treating low pH, ferric iron-dominated ARD, (2) to determine the key geochemical processes controlling the development of the observed trace metal profiles in the pore waters and LBOS relative to the three reaction zones, and (3) to predict the long-term sequestration of trace elements in the LBOS.

Materials and Methods

The experimental set-up employed in this study was described previously (Thomas et al., 1999; Thomas, 2002). Briefly, eight plastic tanks (92 cm diameter by 122 cm tall) were used to simulate vertical flow wetlands. Each vertical flow wetland (VFW) tank was filled with 92 cm of limestone buffered organic substrate (LBOS) overlying 15 cm of coarse (#57; i.e. ~1.27 cm) limestone (Fig. 2a). Composition and physicochemical characteristics of the limestone buffered organic substrate (LBOS) are presented in Table 1.

The ARD was delivered continuously at an average rate of ~20 $mL \cdot min^{-1}$ to the top of each VFW tank for two years, starting in late December 1998 and ending in December 2000 (Thomas, 2002). Effluent drained from the bottom of the tanks through standpipes such that a 15-cm column of ARD was maintained over the LBOS. Influent ARD had an average pH of 2.4 and was dominated by ferric iron (96% Fe^{3+}; 142 $mg \cdot L^{-1}$ total) and aluminum (84 $mg \cdot L^{-1}$) as primary contaminants (Thomas, 2002). The final overall average surface-area acidity loading for all eight tanks was 58 $g \cdot d^{-1} \cdot m^{-2}$ with a range between tank averages of 44 to 76 $g \cdot d^{-1} \cdot m^{-2}$ (Thomas, 2002). For any individual tank occasional high flow rates resulted in acidity loading rates as high as 975 $g \cdot d^{-1} \cdot m^{-2}$ without any significant reduction in the effluent alkalinity.

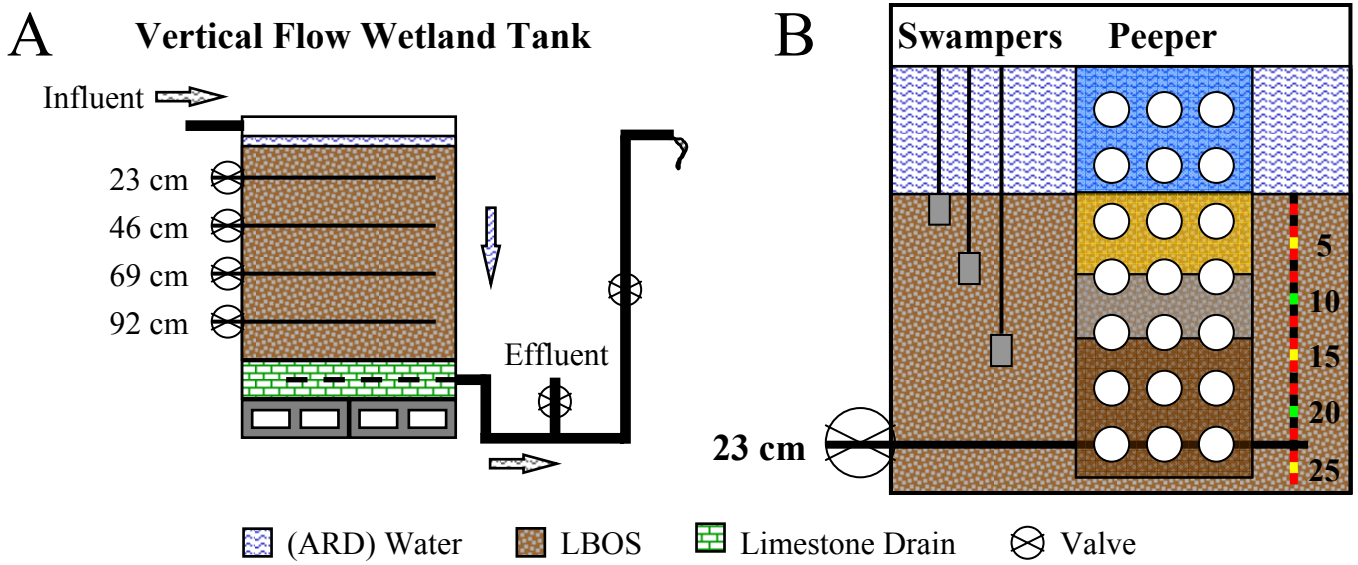

Figure 2. Cross section of the vertical flow wetland (VFW) tank. A. Overview of the tank set up. B. Close-up of susbtrate above 23 cm showing the sampling location of the swamper and peeper pore water samples. The scale to the right is in centimeters.

Table 1. Composition and physicochemical attributes of the limestone buffered organic substrate (LBOS).

LBOS Composition (by volume)	**Physicochemical Attributes**[†]	
	• **CEC:** **83.29 meq·100 gm^{-1} soil**	
	• **NP:** **529 g $CaCO_3$·Kg^{-1} soil**	
• 25% Limestone Screenings • 72% Composted Stable Waste • 3% Spent Brewing Grains • <1% Kricket Krap ®	• **Paste pH 7.61**	• **Carbon 36 %**
	• **Density: 0.741 g·cm^{-3}**	• **C:N 28.8**

all values in mgákg^{-1}	**Fe**	**Al**	**Ca**	**Mn**	**As**	**Cr**	**Cu**	**U**	**Cd**	**Co**	**Ni**	**Zn**
LBOS Total	2805	1611	217048	135	2.5	6.7	4.5	23	0.9	0.9	93	35
Limestone Total	546	543	694339	143	6.0	7.1	1.2	2.5	0.6	2.3	18	4
Limestone Contribution [a]	289	287	367305	76	3.2	3.8	0.6	1.3	0.3	1.2	10	2
Org. Matter Contribution [b]	2516	1324	-	59	-	3.0	3.8	22	0.6	-	84	33

Limestone Screenings - Grain Size Distribution								
(mm)	**9.5 - 4.8**	**4.8 - 2.4**	**2.4 - 1.2**	**1.2 - 0.6**	**0.6 - 0.3**	**0.3 - 0.15**	**0.15 - 0.07**	**< 0.07**
Percent	**2.50%**	**22.2%**	**31.5%**	**27.0%**	**13.4%**	**3.12%**	**0.32%**	**0.03%**

[†] Physicochemical attributes are from Thomas et al. (1999)

[a] Limestone contribution was determined by multiplying the limestone total metal concentration by the proportion of limestone in the LBOS (i.e., 0.529)

[b] Organic matter contribution was determined by difference. Values are not given where the metal concentration measured in the limestone was greater than the concentration measured in the final LBOS.

Water Sampling and Analysis

Acid rock drainage was flushed through the VFW tanks for ~4 months prior to the onset of sampling. A single influent water sample was taken (weekly) from a manifold distributing water to the eight tanks and effluent water samples were taken from each tank from April 1999 to December 2000. To facilitate this study, trace element data were collected as splits from influent, effluent, and pore water samples that were previously characterized for iron, aluminum, and calcium (Thomas, 2002). Fine-scale pore water samples were collected using a vacuum-operated pore-water extractor (i.e., swamper, Winger and Lasier, 1991) and acrylic pore-water diffusion samplers (i.e., peepers, Hesslein, 1976; Carignan, 1984; Carignan et al., 1985).

Pore Water Sampling. Swampers were basically tubes with a filter (e.g., air stone) at one end and connected to a vacuum flask at the other end. The filter-end of the tubing was placed in the soil and a pore water sample was drawn into the flask via a vacuum pump (see Winger and Lasier, 1991; Thomas, 2002 for details). Swamper samples were taken June 2000 from two different VFW tanks (30A and 36A). Three different areas (-1, -2, -3), approximately 120° apart, were sampled in each tank. At each sampling area, pore water was drawn at three depth horizons below the substrate-water interface (6-, 15-, and 23-cm; Fig. 2b). Approximately 100 mL of pore water was recovered at each horizon. Although the swamper sampling depths originally targeted three reaction zones, the final swamper data represented only pore waters of the middle oxide (6 cm) and sulfide (15 and 23 cm) zones. A single sample of the water column above the LBOS was taken with a syringe to represent influent ARD at the time of sampling. In addition, influent ARD from the manifold and effluent water from the respective tanks were collected the day prior to swamper sampling (these data are also plotted on the pore graphs, see below).

The peeper was a made using an acrylic (Plexiglas) plate with wells drilled in it (3cm diameter). The wells were filled with deionized water (~3 mL), covered with a 10 nm polycarbonate dialysis membrane, and secured by another matching plate containing 3 cm holes (Hesslein, 1976; Carignan, 1984; Carignan et al., 1985). The peeper contained a total of seven well horizons that provided a detailed pore water profile of the LBOS. Peeper pore water was collected from one tank (44A) between May 21 and June 6, 2000. The peeper was inserted in the LBOS such that the first two well horizons were situated in the water column above the

LBOS (-7.5 and -2.5 cm) with the bottom edge of the second well horizon positioned at the sediment-water interface (Fig. 2b). The remaining five well horizons provided a pore water profile of the LBOS at 2.5, 7.5, 12.5, 17.5, and 22.5 cm depth. The peeper was left in the LBOS for sixteen days. During this time, the pore water equilibrated with the deionized water through osmosis (Carignan, 1984; Carignan et al., 1985). For the peeper profile, Thomas (2002) determined that the first two well horizons (-7.5 and -2.5 cm) sampled the ARD water column overlying the LBOS. The third well horizon (2.5 cm), which was the first horizon in the substrate, sampled pore waters of the upper portion of the oxide zone. The fourth (7.5 cm) and fifth (12.5 cm) peeper sampling horizons represented the interface of the oxide and transitional zones and the bottom of the transitional zone, respectively, and the lower most two peeper well horizons (17.5 and 22.5 cm) sampled pore waters of the sulfide zone. In addition to the peeper samples, influent ARD from the manifold and effluent water from tank 44A was collected the day prior to peeper insertion and then weekly during the equilibration period (three samples total, which are also plotted on the pore graphs, see below).

Water Analysis. All water samples collected for this study were analyzed for temperature, pH, and dissolved trace metal content (As, Cd, Co, Cu, Ni, U, Zn); further analysis of the same water samples is presented elsewhere (Thomas, 2002). Temperature and pH were measured in the field (Thomas, 2002). Influent, effluent, and swamper samples for dissolved trace-metal analysis were filtered (0.45 μm), while peeper samples did not require filtering due to the 10 nm pore size of the dialysis membrane (Thomas, 2002). All samples for dissolved trace-metal analysis were acid preserved (1% HNO_3) prior to analysis by inductively coupled plasma mass spectrometry (ICP-MS, Elan 6000, Perkin-Elmer Corporation, Norwalk, CT). Instrument precision was generally < 3% and accuracy was within 10% based on second source calibration checks with certified standards. Lower detection limits of the ICP-MS are listed in Table 2 for the individual elements analyzed in this study.

Substrate Sampling and Analysis

Substrate cores were extracted from two tanks (30A and 36A). In each tank, three areas, 120° apart, were sampled in June 2000 followed by a second sampling event in November 2000 at approximately 60° from the first event. Each core sampled approximately ~20 – 25 cm of the

upper LBOS. For the June 2000 sampling, swamper samples were taken concurrently directly adjacent to the cores.

Cores were extruded in an anaerobic glove bag and sectioned lengthwise (Thomas, 2002). Cores were divided according to the three reaction zones based on color and texture (see, Fig. 1). Material from each zone was sealed separately in an air-tight polyethylene bottle under nitrogen, and frozen for later analysis. At a later date, samples were thawed under nitrogen and physically homogenized. A subsample of each reaction zone was chemically analyzed using total dissolution techniques (described below).

Samples of the initial substrate were also collected as the tanks were initially filled with LBOS in the fall of 1998. Each sample was air-dried, homogenized, and stored for later analysis. All samples of the initial LOBS were treated according to the methodologies outlined below for the core samples to provide baseline data on the solid phase.

Total Metal Digests. Five to ten gram splits of each reaction zone from each core were weighed, removed from the nitrogen atmosphere, and air-dried for several days. The air-dried samples were then re-weighed to obtain a gravimetric water content. The dried samples were ground to a fine powder with a cryogenic grinder for total metal analysis. Eight samples of the initial substrate were also cryogenically ground. Approximately 0.5 g of each powdered sample was digested with 10mL of 50% trace-metal grade HNO_3 plus a few drops of 30% H_2O_2 at 105°C using a block digester according to EPA method 3050B for the acid digestion of sediments, sludges, and soils. Method 3050B is an "environmental digest" and does not completely solubilize refractory material such silicates and resistant organic matter. Therefore, small amounts of detritus (i.e., quartz) and clear organic fragments remained after the digest.

The digest was diluted to a final volume of 50 mL with deionized water and then filtered (0.45 μm) before analysis by inductively coupled plasma optical emission spectrometry (ICP-OES, Elan 4300DV, Perkin-Elmer Corporation, Norwalk, CT). Using the gravimetric water content of each sample, the ICP-OES data was back-calculated such that all of the total digest data is given relative to the dry weight of the sample.

The ICP-OES methodology and quality control procedures employed were based on the EPA method 6010 (SW 846). The ICP-OES calculated precision internally by collecting triplicate readings for each sample. The internal relative standard deviation (i.e., instrument precision) of

these readings was usually < 2%. Similar to the ICP-MS procedure, samples were calibrated to certified standards as described above. In an effort to gauge sample heterogeneity and reproducibility (i.e., overall precision), several replicate, 0.5-g powdered samples were digested and analyzed; results were within 20% of each other.

Results and Discussion

Influent – effluent water chemistry.

Influent and effluent chemistry are reported in Table 2. Effluent samples from the tanks indicated that the LBOS was highly effective at removing trace contaminants from low pH, ferric iron-dominated ARD over the two years of the study. In general, for all trace elements, the highest and lowest effluent values recorded for individual tanks were directly related to the fluctuations in influent concentration, so that the highest effluent concentrations occurred concurrent with the highest influent concentrations. To minimize the effect of fluctuations in influent trace element concentration over time, reductions in the trace element concentration were calculated as the percentage of trace element removed (avg. effluent/avg. influent).

The greatest reduction in effluent occurred with copper and cobalt with >99% average removal of both trace metals in all eight tanks. Ninety-nine percent of the influent nickel and 98% of the influent chromium were also removed on average in all eight tanks without significant variation among the tanks. Cadmium removal was consistently below the detection limit of the ICP-MS in all eight tanks. There was slight variation in the range of average uranium and zinc removed among tanks with 97% to >99% uranium and 96 to 98% zinc removed. Finally, arsenic exhibited a 10% range in average removal between tanks with a minimum of 88% and a maximum of 98% for a single tank.

Table 2. Influent and effluent pH and trace metal chemistry for the individual VFW tanks. Values in parenthesis are the range over the 2 year study; where only one value is given, the lower value is below detection limits of the ICP-MS. Data for Ca, Fe, Al, SO_4, and H_2S are from Thomas and Romanek (2002b).

	pH Std Units	Ca (mgáL^{-1})	Fe (mgáL^{-1})	Al (mgáL^{-1})	As (µgáL^{-1})	Cd (µgáL^{-1})	Cr (µgáL^{-1})	Cu (µgáL^{-1})	U (µgáL^{-1})	Co (µgáL^{-1})	Ni (µgáL^{-1})	Zn (µgáL^{-1})	Sulfate (mgáL^{-1})	Sulfide (mgáL^{-1})
L.D.L		0.023	0.00139	0.0026	0.16	0.1	0.82	0.3	0.03	0.07	0.22	0.83	0.5	0.05
Influent	2.4	52	142	84	29.2	6.2	89.8	383	11.6	356	716	1647	1521	n/a
ARD	(1.6 to 3.0)	(23 to 114)	(92 to 237)	(39 to 274)	(134)	(12)	(58 to 188)	(190 to 792)	(22)	(186 to 770)	(377 to 1548)	(741 to 3417)	(926 to 3385)	n/a
Tank 2A	6.48	570	12.9	0.17	2.6	0.10	1.6	0.8	0.1	1.2	6.7	35	1248	1.2
	(5.9 to 6.9)	(268 to 807)	(40)	(9.3)	(16)	(0.2)	(8.7)	(5.4)	(0.5)	(12)	(21)	(154)	(696 to 1817)	(15)
Tank 10A	6.42	611	11.6	0.02	1.2	0.10	2.2	1.2	0.1	1.1	8	45	1275	3.2
	(5.9 to 6.9)	(371 to 1003)	(0.1 to 90)	(0.2)	(6.3)	(0.1)	(39)	(8.9)	(0.7)	(13)	(34)	(174)	(495 to 2732)	(20)
Tank 13A	6.34	610	32.8	0.07	0.7	0.1	1.8	1.6	0.1	1.0	9.4	59	1277	0.7
	(5.5 to 6.9)	(392 to 921)	(0.6 to 123)	(4.2)	(6.9)	(0.2)	(23)	(16)	(0.7)	(7.4)	(72)	(250)	(876 to 1938)	(15)
Tank 24A	6.40	619	16.7	0.03	1.4	0.10	1.5	1.0	0.4	1.1	7.0	47	1273	4.0
	(6.0 to 6.9)	(373 to 888)	(120)	(0.4)	(9.9)	(0.2)	(6.1)	(8.2)	(11)	(7.3)	(22)	(370)	(541 to 2257)	(40)
Tank 30A	6.42	616	14.1	0.02	3.5	0.10	1.5	0.9	0.2	1.2	7.3	44	1302	1.6
	(5.9 to 6.8)	(380 to 943)	(0.01 to 76)	(0.3)	(20)	(0.5)	(7.4)	(7.6)	(5.8)	(15)	(24)	(180)	(678 to 2323)	(15)
Tank 36A	6.33	604	19.2	0.02	1.9	0.10	1.7	1.5	0.1	1.5	9.0	62	1186	2.8
	(5.5 to 6.8)	(372 to 853)	(58)	(0.3)	(13)	(0.1)	(17)	(7.1)	(0.7)	(21)	(44)	(336)	(627 to 2098)	(20)
Tank 39A	6.5	609	2.3	0.02	2.5	0.10	2.1	0.9	0.05	1.3	7.4	33	1113	9.4
	(6.0 to 7.0)	(398 to 915)	(11)	(0.2)	(17)	(0.1)	(15)	(10)	(0.5)	(18)	(25)	(135)	(263 to 1585)	(1 to 30)
Tank 44A	6.50	558	6.8	0.05	2.4	0.10	1.9	1.6	0.1	1.3	9.3	44	936	15.6
	(5.2 to 7.1)	(362 to 907)	(48)	(2.2)	(27)	(0.2)	(8.3)	(10)	(1.6)	(26)	(56)	(148)	(427 to 1569)	(0.1 to 50)
Average	6.42	600	14.5	0.05	2.0	0.10	1.8	1.2	0.13	1.2	8.0	46	1201	4.8
Min	6.33	558	2.3	0.02	0.7	0.10	1.5	0.8	0.05	1.0	6.7	33	936	0.7
Max	6.50	619	32.8	0.17	3.5	0.10	2.2	1.6	0.36	1.5	9.4	62	1302	15.6

L.D.L = lower detection limits of the ICP-MS, n/a = not analyzed
Average, minimum, and maximum were calculated from the individual tank averages

Pore water – swampers and peepers.

The pore water data collected with both the swamper and peeper samplers are presented in Figs. 3, 4, and 6 - 11. In addition to pore water data, the influent ARD, sampled at the distribution manifold, and the effluent, sampled at the standpipe, are also plotted. For the swamper data, two influent and two effluent samples are shown. The influent samples were collected from the manifold eight days prior to and one day before sampling, while the effluent samples were collected, one from each tank, the day before sampling. For the peeper data, there are three influent and three effluent samples shown. Influent and effluent samples were collected the day before the peeper was installed, one week later, and after two weeks concurrent with removal of the peeper sampler.

With the exception of Uranium, the bulk of trace metal removal occurred in the oxide and transitional zones. Details for individual trace elements are presented below.

Total Digest Data

Total digest data are presented in Fig. 4 and Figs. 6 - 11 for core samples from each reaction zone and the initial LBOS. To provide baseline data, total trace element concentrations of the initial LBOS were determined (Figs. 4, 6 - 11; Table 1). Based on the trace element content of the limestone screenings and the known mixing ratio of organic matter to limestone (52.9% $CaCO_3$), the trace element contribution from the limestone was determined (Table 1). The trace element content of the organic matter component was determined by subtracting the limestone contribution from the total (Table 1).

Trends in pH and Individual Trace Elements

pH. Swamper and peeper pore water data (Fig. 3) indicated that the oxide zone (0 – 10 cm deep) yielded a range of pH values that increased with depth from pH 2.3 (2.5 cm) to 3.8 (7.5 cm). The pH continued to increase through the transitional zone (pH 4.6 at 12.5 cm). The 15 and 23 cm swamper sampling depths and the lower two peeper well horizons (17.5 and 22.5 cm), provided 14 samples of the sulfide zone with a fairly narrow pH range (6.8 – 7.6) for all samples. Both pore water analysis techniques indicated that the pH in the sulfide zone was higher than the final effluent values.

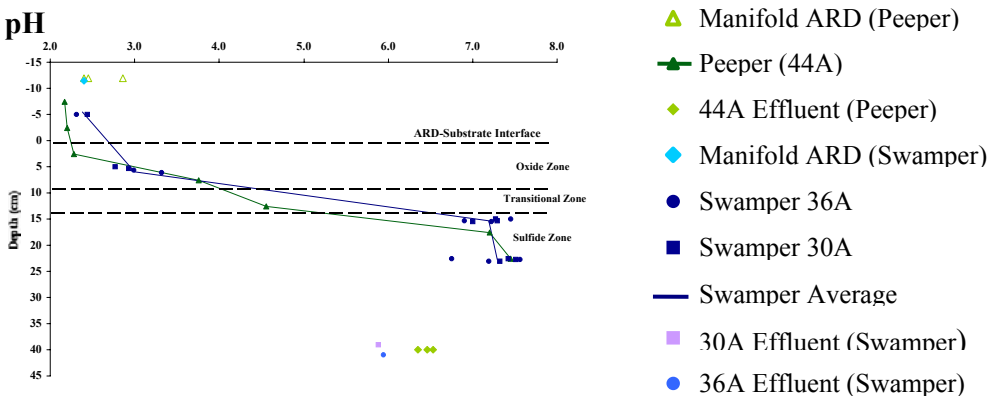

Figure 3. The pH profile of the upper 25 cm of LBOS. The vertical axes are sampling depth; negative values indicate samples were collected from the ARD water column overlying the substrate or the influent. For the swamper samples, individual data points from the two tanks (dark blue circles and squares) are given with an overall swamper average (dark blue line). Influent ARD from the manifold (light green for peeper and sky blue for swamper) and the tank effluent samples (light green for peeper and light blue and lavender for swamper) were collected immediately prior to peeper and swamper sampling (see text for details).

Arsenic. Analysis of arsenic concentrations in the ARD water column overlying the LBOS (8 and 14 $\mu g \cdot L^{-1}$ from tanks 36A and 30A, respectively; Fig. 4) indicated that greater than 85% of the arsenic measured at the ARD source (92 $\mu g \cdot L^{-1}$) was removed at influent pH levels (i.e., 2.2 – 2.4) either in the piping system delivering the ARD to the tank or in the water column overlying the ARD. Total digest data showed that the majority of the arsenic sequestered in the LBOS was retained in the oxide zone (Fig. 4). Arsenic concentrations in oxide zone solids increased an order of magnitude (21 $mg \cdot kg^{-1}$) during the first eighteen months of the project with continued increase over the next six months (35 $mg \cdot kg^{-1}$).

Thomas (2002) demonstrated that iron oxyhydroxide precipitation occurred around the tank inlet (Fig. 5) and within the ARD water column. Because arsenic tends to form oxyanions (e.g., arsenate), which strongly adsorb to iron hydroxy-minerals at low pH (Dzombak and Morel, 1990; McBride, 1994), removal of arsenic was most likely facilitated by the low pH of the ARD water column through adsorption to iron oxyhydroxides.

Given that most of the dissolved arsenic was removed at influent pH through adsorption to iron oxyhydroxides, remobilization was not expected as the pH of the substrate dropped over time. Pore water, which did not show any increase above influent concentrations, and total

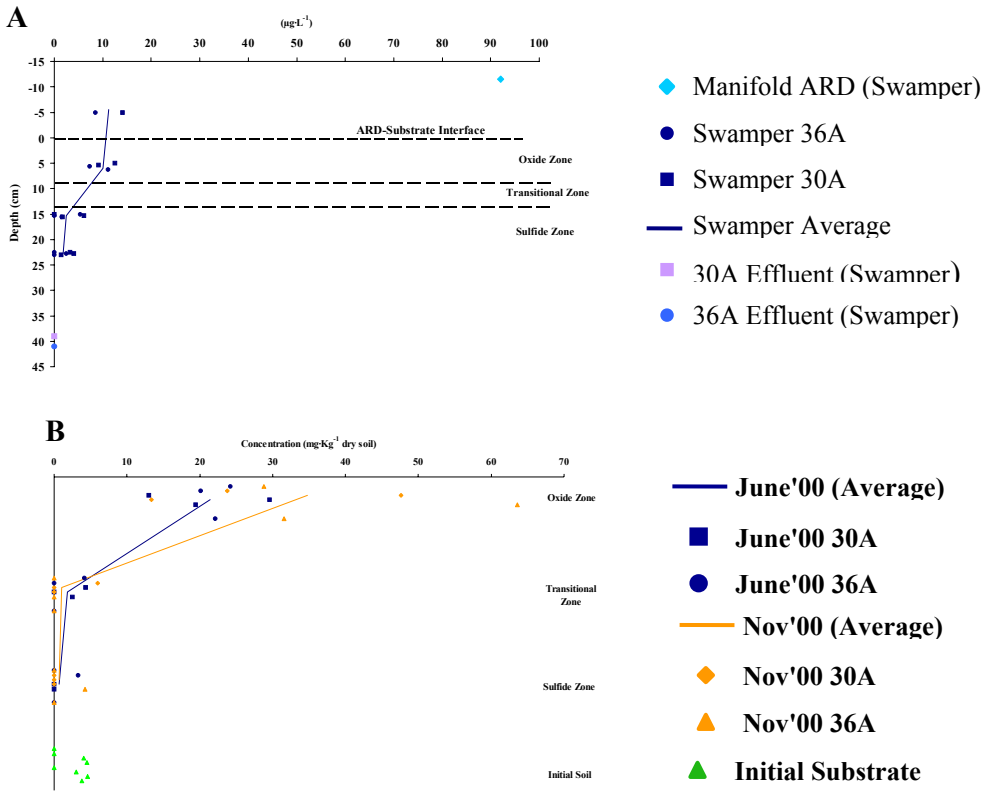

Figure 4. (A) Dissolved arsenic concentrations from the upper 25 cm of the LBOS. The vertical axes are sampling depth; negative values indicate samples were collected from the ARD water column overlying the substrate or the influent. In addition to the individual sampling points from the two tanks (dark blue circles and squares), an overall swamper average is given (dark blue line). Influent ARD from the manifold (sky blue) and the tank effluent samples (light blue and lavender) were collected immediately prior to swamper sampling (see text for details). (B) Total arsenic analysis of LBOS. Data are divided by reaction zone (oxide, transitional, and sulfide), date of collection (blue and orange), and finally by tank (30A or 36A). The lines connect average values for each zone. Eight replicates of the initial substrate are provided (green triangles).

digest data, which did not show any migration of arsenic deeper in the substrate, support this conclusion (Fig. 4). In fact, because arsenic removal through adsorption to iron oxyhydroxides was favored by low pH, decreases in the LBOS pH over time should promote further arsenic removal and prevent any significant mobilization of arsenic.

Figure 5. Photographs of the tank influent orifice showing iron oxyhydroxide crust precipitated at pH ~2.4. These low pH iron oxyhydroxides crusts may have played a significant role in the sorption and retention of arsenic from the influent ARD.

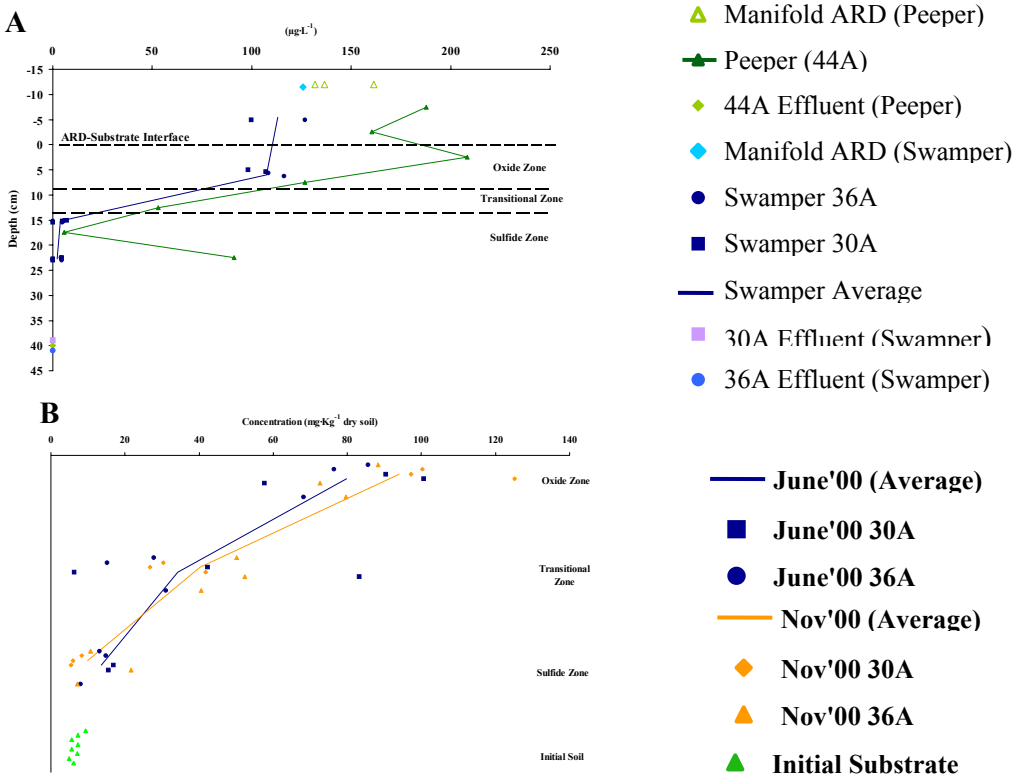

Figure 6. (A) Dissolved chromium concentrations from the upper 25 cm of the LBOS. The vertical axes are sampling depth; negative values indicate samples were collected from the ARD water column overlying the substrate or the influent. For the swamper samples, individual data points from the two tanks (dark blue circles and squares) are given with an overall swamper average (dark blue line). Influent ARD from the manifold (light green for peeper and sky blue for swamper) and the tank effluent samples (light green for peeper and light blue and lavender for swamper) were collected immediately prior to peeper and swamper sampling (see text for details). (B) Total chromium analysis of LBOS. Data are divided by reaction zone (oxide, transitional, and sulfide), date of collection (blue and orange), and finally by tank (30A or 36A). The lines connect average values for each zone. Eight replicates of the initial substrate are provided (green triangles).

Chromium. Swamper and peeper samples of the oxide zone exhibited a range of chromium values that was somewhat pH dependent (Fig. 6). Pore water from the upper oxide zone (pH 2.3), collected at 2.5 cm with the peeper, contained dissolved chromium (208 $\mu g \cdot L^{-1}$) that was higher than the influent concentration, suggesting that chromium previously precipitated at a higher pH was dissolved from the LBOS as the pH approached influent levels. Swamper samples indicated that dissolved chromium in the oxide zone at 6 cm was similar to influent concentrations when the pH was between 2.8 and 3.3. Peeper pore water samples collected from the second well horizon (7.5 cm) indicated minor chromium retention in the bottom of the oxide

zone at pH 3.8 (i.e., 22% of the influent concentration), where pH approximated the pH_{50} for chromium (III) adsorption to iron oxyhydroxide (i.e., between 3.5 and 4.5; Dzombak and Morel, 1990).

Total digests of June 2000 core samples from the oxide zone showed that chromium concentrations increased an order of magnitude (80 $mg \cdot kg^{-1}$ average) compared to the initial LBOS and accounted for most of the chromium removed during the first eighteen months of the project (Fig. 6); solid phase chromium continued to increase over the next six months (94 $mg \cdot kg^{-1}$ average for November 2000 core samples). Therefore, the solubilization of chromium from the upper oxide zone must have been fairly matched by reprecipitation within the lower oxide zone as suggested by the pore water data.

Peeper pore water data also showed that additional chromium removal occurred in the transitional zone (12.5 cm) between pH 3.8 and 4.6. Although pore water data indicated significant chromium precipitation in the transitional zone (pH 3.8 – 4.6), only two thirds of the cores extracted in June 2000 showed significant (greater than a four-fold) increase in total chromium relative to the initial substrate, suggesting chromium precipitation in the transitional zone was recent. November 2000 digests showed that chromium accumulation within the transitional zone continued over time. At pH > 4, chromium may precipitate as insoluble $Cr(OH)_3$; however below pH 4, $Cr(OH)_3$ is highly soluble (Sass, 1987). Therefore, it is likely that chromium was precipitated in the transitional zone as Cr^{3+} sorbed to aluminum hydroxysulfate or $Cr(OH)_3$ precipitated on LBOS surfaces.

The majority of swamper and peeper pore water samples from the sulfide zone (>15 cm) indicated that >96% of the dissolved chromium measured in the ARD water column was removed at pH < 6.8, which is similar to that removed when ratioing the final effluent concentration with the influent concentration (Table 2). As an exception, chromium in the lower most peeper well horizon was ~91 $\mu g \cdot L^{-1}$ at pH 7.4. Therefore, chromium was removed from the pore water prior to reaching the sulfide zone. This is supported by total digest data, which shows that the chromium concentration in the sulfide zone was only slightly higher than the initial substrate and there was little change in the sulfide zone chromium concentration over time.

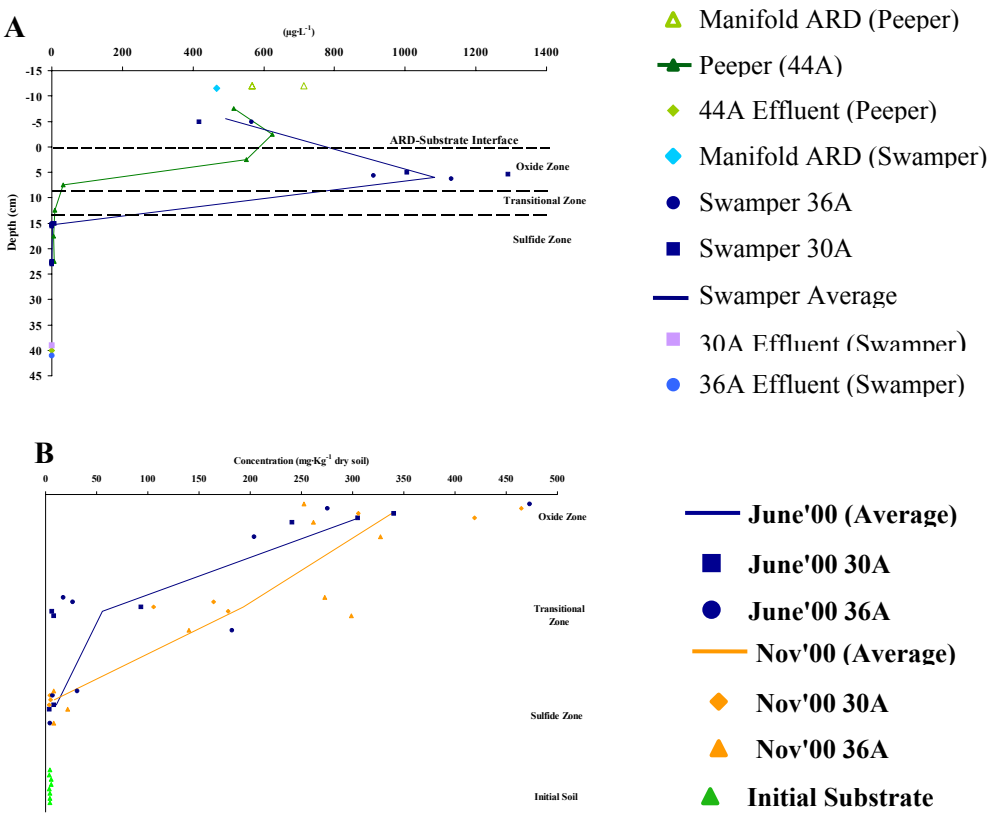

Figure 7. (A) Dissolved copper concentrations from the upper 25 cm of the LBOS. The vertical axes are sampling depth; negative values indicate samples were collected from the ARD water column overlying the substrate or the influent. For the swamper samples, individual data points from the two tanks (dark blue circles and squares) are given with an overall swamper average (dark blue line). Influent ARD from the manifold (light green for peeper and sky blue for swamper) and the tank effluent samples (light green for peeper and light blue and lavender for swamper) were collected immediately prior to peeper and swamper sampling (see text for details). (B) Total copper analysis of LBOS. Data are divided by reaction zone (oxide, transitional, and sulfide), date of collection (blue and orange), and finally by tank (30A or 36A). The lines connect average values for each zone. Eight replicates of the initial substrate are provided (green triangles).

Copper. Of the transitional elements studied, copper has the highest affinity for organic matter (Stumm and Morgan, 1981; McBride, 1994; Sobolewski, 1999; Walton-Day, 1999). Moreover, organically complexed copper is typically bound more tightly than any other divalent transitional metal (McBride, 1994; Sobolewski, 1999). In studies of wetland sediments removing copper, Sobolewski (1999) noted that this strong affinity required harsh chemical treatment for total copper extraction suggesting it was bound to recalcitrant rather than labile organic compounds.

The range in dissolved copper concentrations obtained from the oxide zone was largely pH dependent (Fig. 7). Peeper data showed there was no significant change in the pore water copper concentration in the upper oxide zone (2.5 cm; pH 2.3) compared with the overlying ARD water column (pH 2.2). In contrast, dissolved copper concentrations in swamper samples (6 cm) nearly doubled relative to the influent levels between pH 2.8 – 3.3 with a maximum concentration of 1291 $\mu g \cdot L^{-1}$ obtained at pH 2.9. This suggested that copper, previously precipitated in the oxide zone at higher pH, was resolubilized as the pH dropped below 3.3. The lack of above-influent-copper concentrations at 2.5 cm may be due to the fact that all of the mobile copper previously precipitated had been removed by the time the pH dropped to 2.3. Although previously precipitated copper was dissolved from the upper oxide zone, peeper data from the bottom of the oxide zone (7.5 cm) showed most of the dissolved copper was reprecipitated between pH 3.3 and 3.8 with >90% copper removal from the pore water relative to the influent. Although pore water data indicated copper was being remobilized from the upper oxide zone after eighteen months, copper in digests of June 2000 core samples from the oxide zone increased approximately two orders of magnitude in concentration (305 $mg \cdot kg^{-1}$ average) compared to the initial substrate (Fig. 7). As a consequence of this recycling of copper within the oxide zone, digest data do not exhibit any discernible temporal changes in total copper over time and therefore give no indication as to the magnitude of copper mobility below pH 3.3. In fact, total digests of core material sampled in November 2000 indicated a slightly higher average copper concentration in the oxide zone (338 $mg \cdot kg^{-1}$) compared to June 2000 cores.

While the bulk of copper was removed in the oxide zone, according to peeper data (Fig. 7), the remaining copper was removed in the transitional zone (12.5 cm) to near effluent concentrations by pH 4.6. Two thirds of the June 2000 transitional zone digest samples contained copper concentrations similar to the initial LBOS (6 – 26 $mg \cdot kg^{-1}$), while the remaining samples showed significant increase (94 and 182 $mg \cdot kg^{-1}$). Digests of November 2000 samples exhibited an increase in total copper (192 $mg \cdot kg^{-1}$) approximately 3.5 times greater than cores collected in June 2000. Moreover, the highest values in the range (105 – 299 $mg \cdot kg^{-1}$) were within the range of copper concentrations observed in the oxide zone. The large increase in copper concentration between June and November 2000 transitional zone samples suggest that copper removal was shifting from total removal in the lower oxide zone to greater removal in the transitional zone. This increase was likely due to the binding of copper with organic matter.

There was only minimal dissolved copper (0 – 8 $\mu g \cdot L^{-1}$) detected in the sulfide zone pore water (> 15 cm) collected with either technique or in the corresponding effluent samples and digests of the sulfide zone produced similar or only slightly elevated copper concentrations compared to the initial LBOS (average 11 $mg \cdot kg^{-1}$).

Uranium. Total digests showed that the LBOS originally contained a significant amount of uranium (23 $mg \cdot Kg^{-1}$) that was largely associated with the organic component (Table 1). The limestone component of the LBOS contributed only ~ 1 $mg \cdot kg^{-1}$ of the total uranium measured in the initial substrate.

Pore water collected from the oxide zone with the swamper (6 cm; pH 2.8 – 3.3) yielded uranium concentrations higher than the ARD overlying the substrate (23 – 32 $\mu g \cdot L^{-1}$), suggesting mobilization of existing uranium solids (Fig. 8). This is corroborated by totals from the June 2000 oxide zone core samples, which displayed a four-fold decrease in uranium concentration over the initial LBOS (6 $mg \cdot kg^{-1}$ average). Totals from the November 2000 cores did not differ significantly from those collected in June 2000 (Fig. 8).

The majority of June 2000 transitional zone core samples exhibited a range of values from 24 to 31 $mg \cdot kg^{-1}$ similar to initial LBOS concentrations, with one exception (80 $mg \cdot kg^{-1}$). There was a significant decrease in uranium between June (36 $mg \cdot kg^{-1}$) and November (9 $mg \cdot kg^{-1}$) 2000 sampling events. In fact, the values from the November 2000 samples were more similar to the oxide zone samples than the June 2000 samples (Fig. 8).

Total digests suggested that uranium was solubilized from the transitional zone over time based on the significant decrease in uranium between June (36 $mg \cdot kg^{-1}$) and November (9 $mg \cdot kg^{-1}$) 2000 sampling events. Unfortunately, pore water data were not available for the transitional zone.

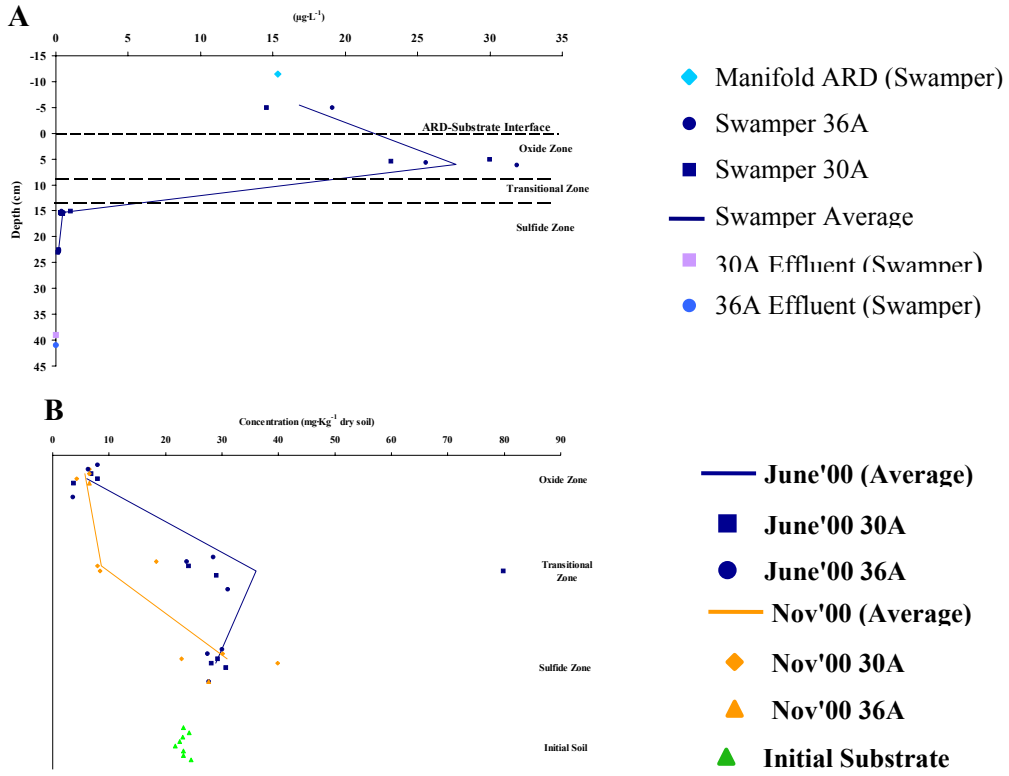

Figure 8. (A) Dissolved uranium concentrations from the upper 25 cm of the LBOS. The vertical axes are sampling depth; negative values indicate samples were collected from the ARD water column overlying the substrate or the influent. In addition to the individual sampling points from the two tanks (dark blue circles and squares), an overall swamper average is given (dark blue line). Influent ARD from the manifold (sky blue) and the tank effluent samples (light blue and lavender) were collected immediately prior to swamper sampling (see text for details). (B) Total uranium analysis of LBOS. Data are divided by reaction zone (oxide, transitional, and sulfide), date of collection (blue and orange), and finally by tank (30A or 36A). The lines connect average values for each zone. Eight replicates of the initial substrate are provided (green triangles).

Swamper samples from the sulfide zone (15 and 23 cm) indicated that uranium was completely removed from the pore water by pH 6.8 (Fig. 8), as concentrations were largely similar to the effluent concentrations (although uranium levels as high as 1 $\mu g \cdot L^{-1}$ were measured). Moreover, total uranium in June 2000 cores from the sulfide zone was slightly higher than the initial substrate with uranium concentrations falling in a fairly narrow range (27 – 31 $mg \cdot kg^{-1}$). Comparison of totals from the June and November 2000 sampling events revealed no difference in average content (29 and 31 $mg \cdot kg^{-1}$, respectively), although the range of values was larger in November 2000 (23 – 40 $mg \cdot kg^{-1}$).

The depletion of uranium from the oxide and transitional zones and apparent accumulation in the sulfide zone is analogous to the formation of uranium roll front deposits (Nash et al., 1981; Langmuir, 1997). The formation of roll fronts can be summarized as follows: trace amounts of uranium are leached from reduced sediments (e.g., LBOS organic material), by oxidized water (e.g., ferric-iron dominated influent ARD). Uranium is transported as the uranyl ion (UO_2^{2+}) under oxidizing and mildly acidic conditions. When the uranyl-bearing water encounters a redox interface, such as the boundary between the transitional zone and the sulfide zone (based on the presence/absence of active sulfide precipitation, i.e., Thomas, 2002), U(VI) is reduced to U(IV) and precipitated as a solid such as pitchblende [$UO_{2(am)}$] (Langmuir, 1997). Reduction is typically accomplished by reaction with organic carbon, S^{2-}, or solid sulfides (Nash et al., 1981).

Uranium accumulation in the sulfide zone was apparently slow based on the small average increase relative to the initial substrate and the lack of a measurable difference between cores collected in June and November 2000. The slow accumulation was likely due to the low level of dissolved uranium measured in the influent (22 $\mu g \cdot L^{-1}$ maximum) and the relatively small amount that resided in the initial LBOS.

In the LBOS, pore water data suggested that uranium mobility was related to pH changes in the oxide zone. However, development of the oxide zone resulted from the ingress of fairly oxidizing ARD (i.e., ferric iron-dominated). Therefore, uranium inherited from the initial substrate was oxidatively leached from the oxide zone and, based on total digest data, from the transitional zone over time. This solubilized uranium, coupled with influent-ARD uranium, was then precipitated, initially in the transitional zone. However, as oxidizing fluids penetrated into the transitional zone, uranium was again mobilized and ultimately accumulated in the sulfide zone. Hence, no uranium retention is expected in the oxide and transitional zones; all of the uranium is predicted to migrate in advance of the limestone dissolution front (i.e., in the sulfide zone) and may accumulate over time. A large spike of dissolved uranium in the effluent would be the first indication that the transitional zone (i.e., limestone dissolution front) is about to break through the LBOS.

Cadmium. Swamper and peeper pore water data displayed different cadmium profiles (Fig. 9). On average, the swamper data showed that the oxide zone (6 cm) cadmium concentrations increased four-fold (39 $\mu g \cdot L^{-1}$). Increases were pH-dependent with average increases between

pH 2.8 – 3.0 (i.e. 33 – 37 $\mu g \cdot L^{-1}$) and a maximum increase (51 $\mu g \cdot L^{-1}$) at pH of 3.3. The increases in cadmium concentrations above influent levels at pH <3.3 indicated that previously precipitated cadmium was dissolved from the upper oxide zone, but precipitated above pH 3.3 in the lower oxide and/or transitional zones (Fig. 9).

In contrast, the peeper data showed there was no significant change in the pore water cadmium concentration in the upper oxide zone (at pH 2.3) compared with the overlying ARD water column (pH 2.2) and therefore apparently exhibited no dissolution of previously precipitated cadmium solids in the upper oxide zone (Fig. 9). Moreover, peeper data showed >50% removal of water column cadmium by pH 3.8 (bottom of the oxide zone) and complete removal by the transitional zone (pH 4.6). However, the validity of the peeper data is questionable due to the lack of cadmium in the influent during the week prior to and the first week of peeper equilibration; the influent cadmium concentration was below the detection limit the week prior to and during the first week of peeper equilibration, while it increased to ~9 $\mu g \cdot L^{-1}$ by the last week of peeper equilibration. The ARD water-column cadmium measured with the peepers ranged between ~12 and 14 $\mu g \cdot L^{-1}$.

In fact, the entire dissolved cadmium profile measured with the peeper may only represent solubilization of previously precipitated cadmium. Consequently, relative to the peeper influent concentration measured at the end of equilibration, the pore water profile may be shifted to lower concentrations due to the lack of influent cadmium. Thus, a pH range more precise than the 3.3 – 6.5 range for the bulk of cadmium precipitation cannot be ascertained. It is noteworthy that: 1) the average influent cadmium concentration was the lowest of the trace elements studied, 2) it was one of only three trace elements (arsenic, cadmium, and uranium) in the influent ARD recorded below detection over the course of this study, and 3) it was the only trace element studied that was below detection during either pore water sampling events.

The majority of cadmium removed in the LBOS for the first 18 months of the project (June 2000 cores) occurred in the oxide zone (Fig. 9); cadmium concentrations exhibited a one and a half order of magnitude increase (22 – 56 $mg \cdot kg^{-1}$ range) compared to the initial LBOS (40 $mg \cdot kg^{-1}$ average). However, totals from the November 2000 cores suggested that cadmium concentration in the oxide zone did not change significantly during the six months between core sampling events (Fig. 9). Cadmium removal in the oxide zone was likely due to coprecipitated

with amorphous and/or crystalline iron oxyhydroxides or complexed with labile organic matter (see Thomas, 2002 for details).

Although pore water data suggested solubilization of cadmium from the upper oxide zone (>6 cm; Fig. 9), core data also showed the highest cadmium concentration of three zones investigated. One possible explanation for the positive correlation between pore water and solids is that cadmium dissolved from the upper oxide zone at pH <3.3 was reprecipitated in the lower oxide zone at a slightly higher pH (3.8) and therefore cadmium was recycled internally within this zone. Alternatively, the amount of variability in oxide zone cadmium totals between cores (June and November 2000) may mask any changes over time. The variability in the total cadmium concentration was most likely attributable to the frequent paucity in influent dissolved cadmium over the course of the project, as the measured concentration was commonly below the ICP-MS lower detection limit (Table 2). Therefore, it can not be determined if the apparent equality in oxide zone cadmium between June and November 2000 was due to internal recycling of cadmium within the oxide zone or if the decreases were so subtle that they were masked by the variability.

Total digests of the June 2000 samples from the transitional zone, which showed only minor accumulations of cadmium (2.7 $mg \cdot kg^{-1}$ average, 1.0 – 5.7 $mg \cdot kg^{-1}$ range; Fig. 9) compared to the initial LBOS, further suggest that cadmium precipitation was focused in the oxide zone during the first eighteen months of the project. In contrast, while pore water data could not distinguish between precipitation in the lower oxide or transitional zone, total digests of November 2000 samples, which displayed significant cadmium precipitation, indicated the majority of cadmium precipitation occurred in the transitional zone during the last six months of the project. This can be attributed to cadmium weakly adsorbed to iron oxyhydroxides found in minor abundance or, more likely, adsorption/coprecipitation with the ubiquitous aluminum hydroxysulfates and/or iron (mono)sulfides.

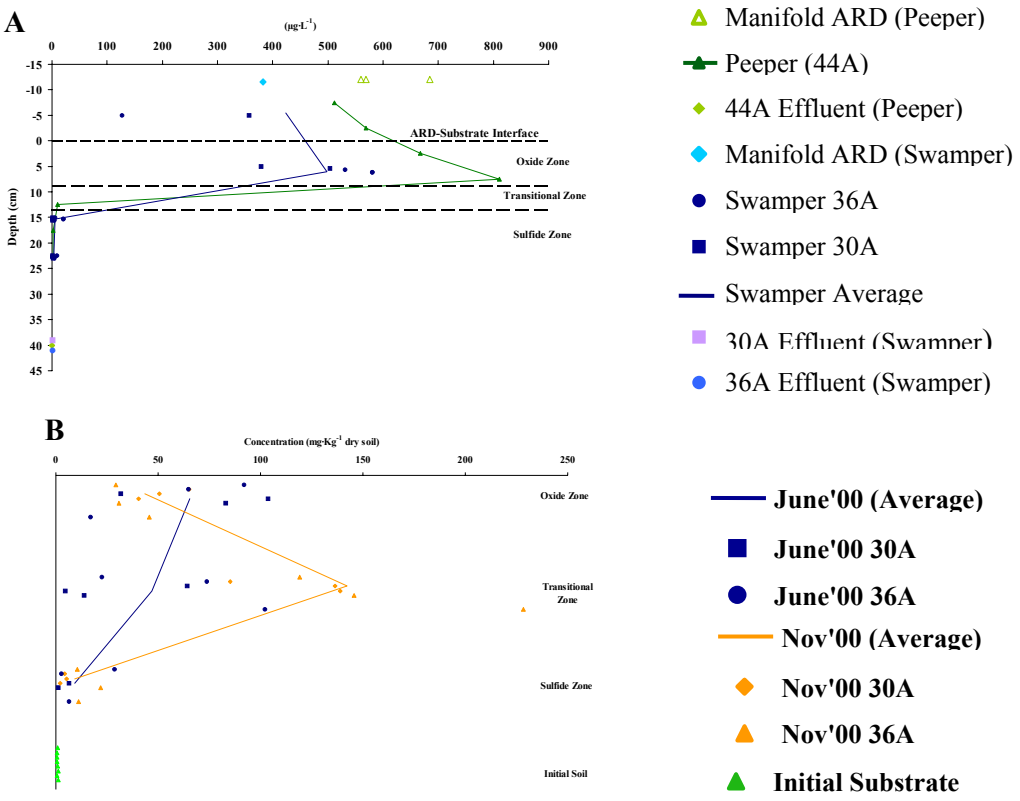

Figure 10. (A) Dissolved cobalt concentrations from the upper 25 cm of the LBOS. The vertical axes are sampling depth; negative values indicate samples were collected from the ARD water column overlying the substrate or the influent. For the swamper samples, individual data points from the two tanks (dark blue circles and squares) are given with an overall swamper average (dark blue line). Influent ARD from the manifold (light green for peeper and sky blue for swamper) and the tank effluent samples (light green for peeper and light blue and lavender for swamper) were collected immediately prior to peeper and swamper sampling (see text for details). (B) Total cobalt analysis of LBOS. Data are divided by reaction zone (oxide, transitional, and sulfide), date of collection (blue and orange), and finally by tank (30A or 36A). The lines connect average values for each zone. Eight replicates of the initial substrate are provided (green triangles).

Cobalt, Nickel, Zinc. Cobalt, nickel, and zinc concentrations all exhibited similar behaviors both within swamper and peeper pore water and total digest profiles (Figs. 10 - 12). Pore water data showed that, in June 2000, cobalt, nickel, and zinc were liberated from the oxide zone (0 – 10 cm) below pH 3.8 and largely reprecipitated in the transitional zone (12.5 cm) between pH 3.8 – 4.6. However, total digests of cores taken concurrently (June 2000) indicated that a significant amount of oxide zone cobalt, nickel, and zinc, previously precipitated at higher pH remained

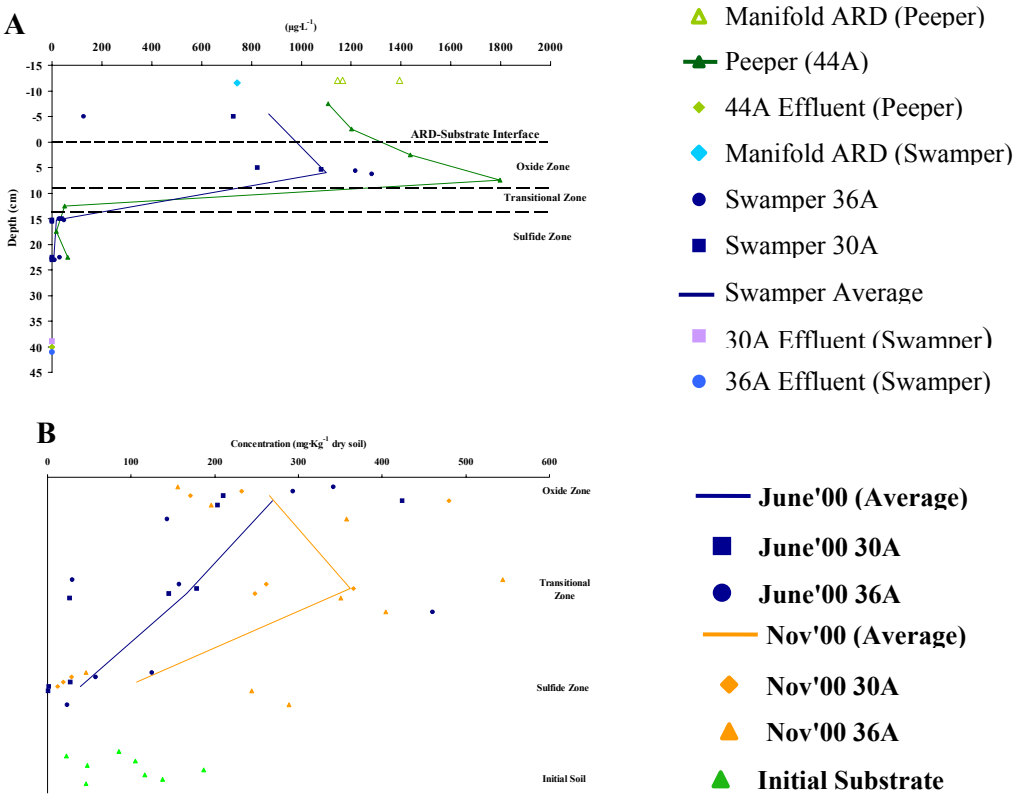

Figure 11. (A) Dissolved nickel concentrations from the upper 25 cm of the LBOS. The vertical axes are sampling depth; negative values indicate samples were collected from the ARD water column overlying the substrate or the influent. For the swamper samples, individual data points from the two tanks (dark blue circles and squares) are given with an overall swamper average (dark blue line). Influent ARD from the manifold (light green for peeper and sky blue for swamper) and the tank effluent samples (light green for peeper and light blue and lavender for swamper) were collected immediately prior to peeper and swamper sampling (see text for details). (B) Total nickel analysis of LBOS. Data are divided by reaction zone (oxide, transitional, and sulfide), date of collection (blue and orange), and finally by tank (30A or 36A). The lines connect average values for each zone. Eight replicates of the initial substrate are provided (green triangles).

(Figs. 10 - 12). In the six months between the June and November 2000 sampling events, the cobalt, nickel, and zinc concentrations in the transitional zone exceeded the concentrations accumulated in the oxide zone during the first eighteen months of the project. Furthermore, for any given core, total cobalt and zinc concentrations in the oxide zone decreased over time; however due to the high degree of variability in nickel concentrations from the initial LBOS, decreases in nickel over time were less apparent. This shows that not only did the site of precipitation shift completely to the transitional zone, but also cobalt, nickel, and zinc

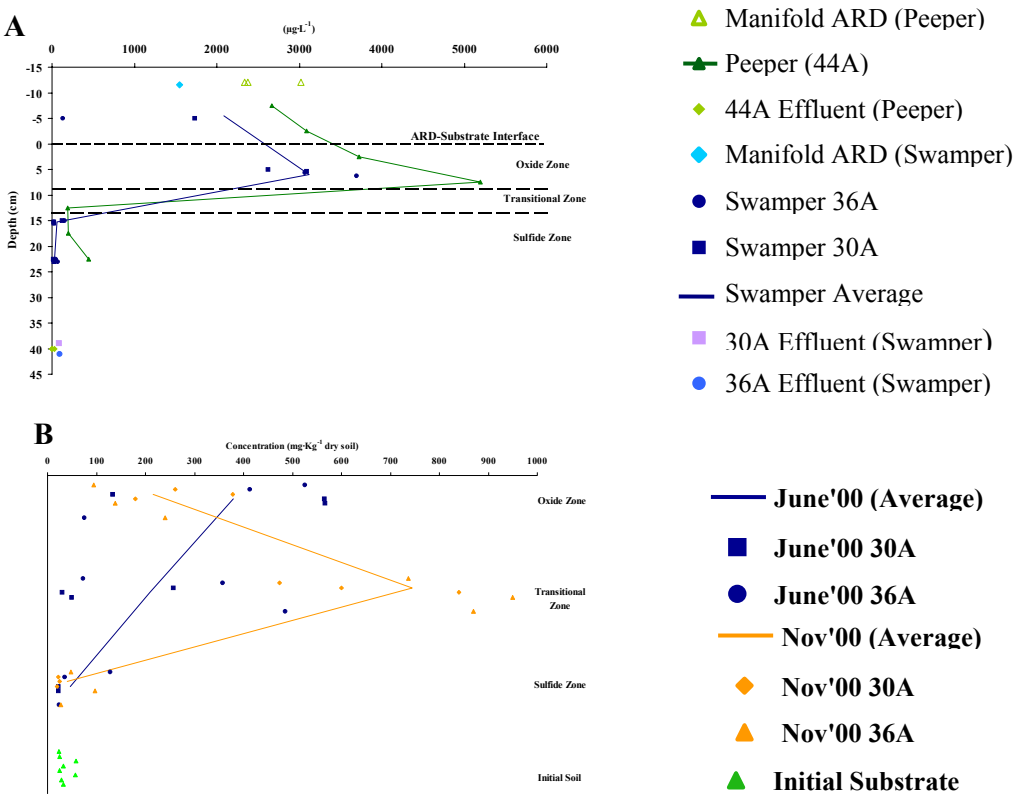

Figure 12. (A) Dissolved zinc concentrations from the upper 25 cm of the LBOS. The vertical axes are sampling depth; negative values indicate samples were collected from the ARD water column overlying the substrate or the influent. For the swamper samples, individual data points from the two tanks (dark blue circles and squares) are given with an overall swamper average (dark blue line). Influent ARD from the manifold (light green for peeper and sky blue for swamper) and the tank effluent samples (light green for peeper and light blue and lavender for swamper) were collected immediately prior to peeper and swamper sampling (see text for details). (B) Total zinc analysis of LBOS. Data are divided by reaction zone (oxide, transitional, and sulfide), date of collection (blue and orange), and finally by tank (30A or 36A). The lines connect average values for each zone. Eight replicates of the initial substrate are provided (green triangles).

previously precipitated in the oxide zone must have been dissolved and relocated in the transitional zone. As with almost all trace elements studied, pore water data showed that cobalt, nickel, and zinc were largely removed above the limestone dissolution front, prior to the sulfide zone (Figs. 10 - 12). Therefore, total digests of the sulfide zone core samples showed only minor increases in total cobalt, nickel, or zinc with little change over time. Cobalt, nickel, and zinc coprecipitation with acid volatile sulfide and pyrite has been previously documented (Huerta-Diaz et al., 1993; McBride, 1994; Huerta-Diaz et al., 1998) and, albeit rare, cobalt-, nickel-, and zinc-bearing sulfides were identified during electron microprobe analysis (see Thomas, 2002).

CONCLUSIONS

Few studies of passive treatment systems have addressed trace element removal during acid neutralization, although elevated levels of some trace elements are commonly encountered in coal-related ARD (e.g., As, Cd, Co, Cr, Cu, Ni, Zn; (Hyman and Watzlaf, 1995). Results from this study show that, for the practical purpose of implementing LBOS to treat low pH, ferric iron-dominated ARD, high trace element removal efficiency can be expected as long as the limestone dissolution front does not pass completely through the substrate. With the exception of uranium, trace metal attenuation largely occurs above the limestone dissolution front in the transitional and oxide zones.

Trace metal removal exhibits a strong dependence on pH. Only arsenic is retained at influent pH values. All other trace elements require an increase in pH to at least 3.3 before they are sequestered. Therefore, trace element removal is confined to either the lower oxide zone concomitant with ferric iron precipitation (pH 3.3 – 3.8; Thomas, 2002) or the transitional zone concurrent with aluminum hydroxysulfate precipitation (pH 3.8 – 4.6; Thomas, 2002). Based largely on pH considerations, the trace metal removal selectivity within the LBOS follows the sequence:

$$As > Cu > Cr > Co = Ni = Zn = Cd > U.$$

Given the pH constraints, only a portion of the dissolved copper and chromium are actively sequestered in the lower oxide zone, while the remaining copper and chromium, cadmium, cobalt, nickel, and zinc are sequestered in the transitional zone. Uranium, which is more dependent on the redox conditions of the LBOS than the pore water pH, is not removed from the pore water until the sulfide zone. Because the location of the transitional zone within the LBOS is dynamic depending on the depth of the limestone dissolution front, the site of active trace element sequestration (i.e., pH > 3.3) is constantly migrating deeper into the LBOS over time. Thus, if the LBOS is implemented to the point where the limestone dissolution front is permitted to pass completely through the substrate and the neutralization potential is completely consumed,

then trace elements (except arsenic) can no longer be sequestered and will pass through the substrate.

However, of greater concern is the fate of trace elements precipitated behind the limestone dissolution front after all of the neutralization potential has been consumed. Results from this study show that all trace elements sequestered at pH > 3.3 are subject to remobilization as the pH decreases over time, although the degree of mobilization is trace element-dependent. These remobilized trace elements coupled with influent concentrations may accumulate in solution at the pH-dependent point of maximum mobility. If the LBOS continues to receive ARD after the limestone dissolution front passes completely through the substrate, dissolved trace elements (with the exception of arsenic) will be released in the effluent as the pH drops to influent levels and at concentrations potentially orders of magnitude higher than the influent concentration. Based on the pH of solubilization and the amount of total trace element solubilized, the following general order of trace element mobility can be applied to the LBOS:

$$U > Co = Zn \geq Cd = Ni > Cu > Cr > As$$

Acknowledgements

This research was funded by Financial Assistance Award Number De-FC09-96SR18546 between the United States Department of Energy and The University of Georgia as a part of the US DOE National Water Research Center. The authors would like to thank the principle investigators of this grant, Dr. Rebbecca Sharitz, Dr. J Vaun McArthur, and Dr. Beverly Collins for their continued support and assistance. The authors would also like to acknowledge Linda Paddock, Daniel Coughlin, Matt Opdyke, and Morris Jones for their technical assistance in sample and chemical analysis.

Literature Cited

Blowes D. W. and Ptacek C. J. (1994) Acid-neutralization mechanisms in inactive mine tailings. In *The Environmental Geochemistry of Sulfide Mine-Wastes, Short Course Handbook*, Vol. 22 (ed. J. L. Jambor and D. W. Blowes), pp. 271 - 292. Mineralogical Association of Canada.

Carignan R. (1984) Interstitial water sampling by dialysis: Methodoligical notes. *Limnol. Oceanogr.* **29**(3), 667-670.

Carignan R., Rapin F., and Tessier A. (1985) Sediment porewater sampling for metal analysis: A comparison of techniques. *Geochimica Cosmochimica et Acta* **49**, 2493-2497.

Dzombak D. A. and Morel F. M. M. (1990) *Surface Complexation Modeling - Hydrous Ferric Oxide*. John Wiley and Sons.

Hesslein R. H. (1976) An in situ sampler for close interval pore water studies. *Limnol. Oceanogr.* **21**, 912-914.

Huerta-Diaz M. A., Carignan R., and Tessier A. (1993) Measurement of trace metals associated with acid volatile sulfides and pyrite in organic freshwater sediments. *Environmental Science and Technology* **27**, 2367 - 2372.

Huerta-Diaz M. A., Tessier A., and Carignan R. (1998) Geochemistry of trace metals associated with reduced sulfur in freshwater sediments. *Applied Geochemistry* **13**, 213 - 233.

Hyman D. M. and Watzlaf G. R. (1995) Mine Drainage Characterization for the Successful Implementation of Passive Treatment Systems. *17th Annual National Association of Abandoned Mine Lands Conference*, 170 - 185.

Hyman D. M. and Watzlaf G. R. (1997) Metals and Other Components of Coal Mine Drainage as Related to Aquatic Life. *National Meeting of the American Society of Surface Mining and Reclamation*.

Kepler D. A. and McCleary E. C. (1994) Successive alkalinity-producing systems (SAPS) for the treatment of acidic mine drainage. *Proc. Int. Land Reclamation and Mine Drainage Conference and Third Int. Conference on the Abatement of Acidic Drainage*, 195-204.

Langmuir D. (1997) *Aqueous Environmental Geochemistry*. Prentice Hall.

McBride M. B. (1994) *Environmental Chemistry of Soils*. Oxford University Press.

Nash J. T., Granger H. C., and Adams S. S. (1981) Geology and concepts of genesis of important types of uranium deposits. *Economic Geology* **75th ann. vol**, 63 - 116.

Sass B. M. a. D. R. (1987) Solubility of amporphous chromium(III)-iron(III) hydroxide solid solutions. *Inorganic Chemistry* **26**, 2228 - 2232.

Smith K. S. (1999) Metal sorption on mineral surfaces - An overview with examples relating to mineral deposits. In *The Environmental Geochemistry of Mineral Deposits, Part A: Processes, Techniques, and Health Issues*, Vol. 6A (ed. G. S. Plumlee and M. K. Logsdon), pp. 161 -182. Society of Economic Geologists.

Sobolewski A. (1999) A review of processes responsible for metal removal in wetlands treating contaminated mine drainage. *International Journal of Phytoremediation* **1**(1), 19 - 51.

Stumm W. and Morgan J. J. (1981) *Aquatic Chemistry*. John Wiley & Sons.

Thomas R. C. (2002) Passive treatment of low-pH, ferric iron-dominated acid rock drainage. *Ph.D. dissertation*, University of Georgia, 365 pp.

Thomas R. C., Romanek C. S., Coughlin D. P., and Crow D. E. (1999) Treatment of acid mine drainage using anaerobic constructed treatment wetlands: predicting longevity with substrate neutralization potential. *Proceedings Sudbury '99 - Mining and the Environment II*, 449-458.

U.S. Code of Federal Regulations. (1991) Title 40 -- Protection of the Environment; Chapter I -- Environmental Protection Agency; Subchapter N -- Effluent Guidelines and Standards; Part 434 - Coal mining point source category; July 1.

Walton-Day K. (1999) Geochemistry of the processes that attenuate acid mine drainage in wetlands. In *The Environmental Geochemistry of Mineral Deposits, Part A: Processes, Techniques, and Health Issues*, Vol. 6A (ed. G. S. Plumlee and M. K. Logsdon), pp. 215 - 228. Society of Economic Geologists.

Watzlaf G. R. (1997) Passive treatment of acid mine drainage in down-flow limestone systems. *Proceedings of the 14th Annual National Meeting of the American Society of Surface Mining and Reclamation.*, 611-622.

Winger P. V. and Lasier P. J. (1991) A vacuum-operated pore-water extractor for estuarine and freshwater sediments. *Arch. Environ. Contam. Toxicol.* **21**, 321-324.